Chapter 4

Spin dilution through biosynthetically site-directed ^{13}C labelling

4.1 Introduction

By exploiting the biosynthetic pathways of amino-acids in bacteria, it results that it is possible to incorporate ^{13}C labels into some sites of the proteins, while leaving other sites unlabelled. Under aerobic conditions, bacteria can utilize glucose or glycerol as the sole carbon source to synthesize the 20 amino-acids[1,2]. Proteins expressed in bacterial systems can be labelled selectively and extensively with ^{13}C by using selectively labelled glucose or glycerol in the protein expression medium[3,4]. The selective and extensive labelling method relies on the specificity of the amino-acid biosynthetic pathway. The ^{13}C enrichment that results, presents several advantages that can be exploited for structure determination of proteins by solid-state MAS NMR. First, there is an improvement in resolution because of the reduced or completely removed line-broadening due to one-bond ^{13}C-^{13}C scalar coupling. The *J*-coupling cannot be removed by magic-angle spinning and in fully ^{13}C-labelled proteins this causes significant line-broadening (see 4.3). Furthermore, in uniformly labelled preparations, the weak ^{13}C-^{13}C dipolar couplings, that reflect long-range distances, are obscured by the strong couplings of directly bonded ^{13}C spins. This occurs because of dipolar truncation and spin-diffusion mechanisms within the dense ^{13}C network[5,6] (see Fig. 3.1). The reduced labelling allows to detect weak couplings between carbon spins close in space but not chemically bonded, which contain the relevant structure information. Finally, the dilution of ^{13}C simplifies the NMR spectra and facilitates the assignment of the now detectable long-range correlation cross-peaks[7].

4.2 [2-^{13}C]glycerol-made SH3 and [1,3-^{13}C]glycerol-made SH3

4.2.1 Prediction of the ^{13}C labelling by following the biosynthetic pathways in bacteria

In the case of our model system α-spectrin SH3 domain, two different samples are prepared, which show complementary labelling schemes obtained by using [2-^{13}C] glycerol or [1,3-^{13}C] glycerol as the sole carbon source in the protein expression media. The resulting ^{13}C enrichment is both extensive and reduced and we refer to the two samples as 2-SH3 and 1,3-SH3, respectively[7].

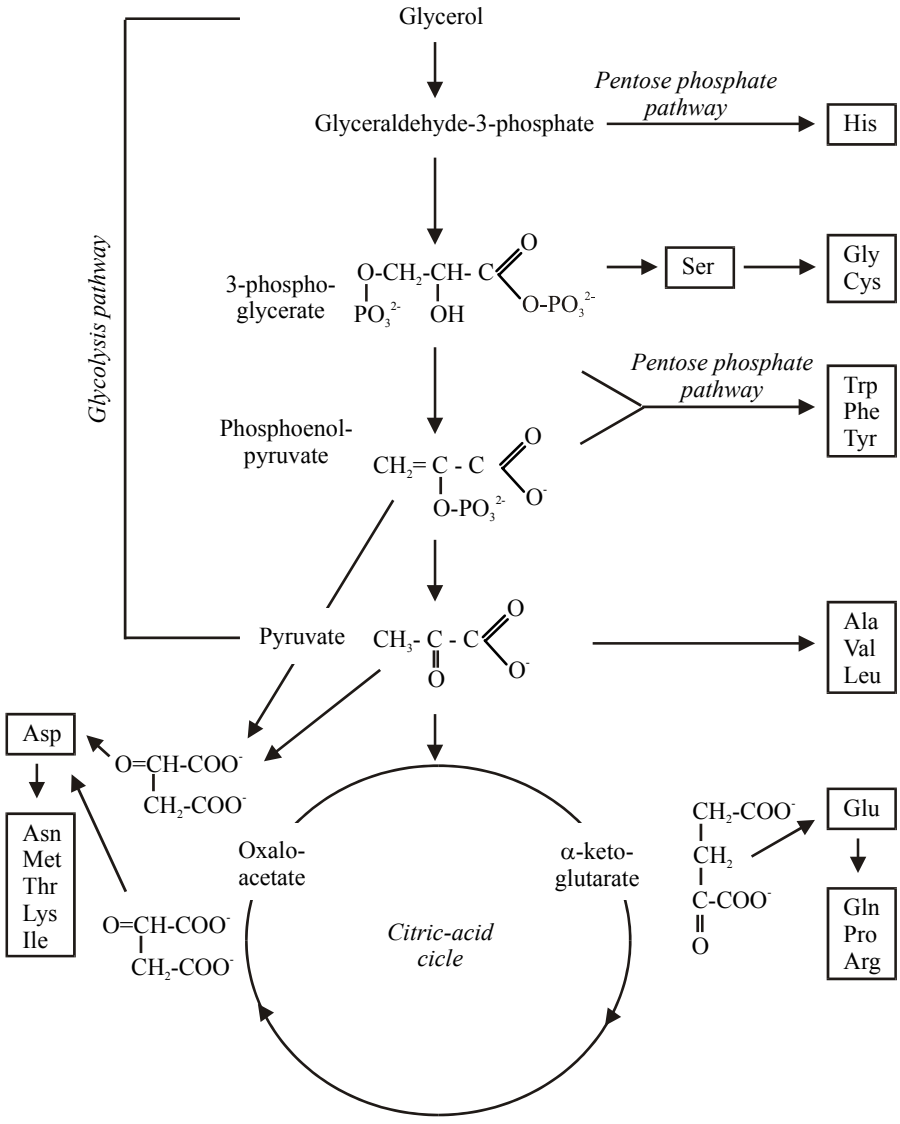

Fig. 4.1 Amino-acid biosynthetic pathway in bacteria, utilizing glycerol as the sole carbon source. The compounds precursors of the 20 amino-acids are shown.

To estimate the ^{13}C-labelled nuclei in the different residues of our protein preparations, the pathway of biosynthetic reactions that produce the different amino-acids was followed,

starting with [2-^{13}C]glycerol or [1,3-^{13}C]glycerol. In Fig. 4.1, a summary of the biosynthetic reactions in bacteria is shown, that comprises three major enzymatic phases: the glycolysis pathway, the pentose phosphate pathway and the citric-acid cycle[1,2]. The 20 amino-acids can be divided into two groups, reflecting the two major steps in the biosynthetic pathway. In the first group, there are 10 amino-acids synthesised from precursors made in the linear enzymatic reactions (which comprise the glycolysis pathway and the pentose phosphate pathway). The second group includes the other 10 amino-acids produced from precursors made in the cyclical reactions of the citric-acid cycle. In Fig. 4.2, the two groups of amino-acids are shown, together with the effective ^{13}C enrichment, as obtained by protein expression starting with [2-^{13}C]glycerol or [1,3-^{13}C]glycerol[7]. The red colour corresponds to the degree of ^{13}C labelling obtained by growth on [2-^{13}C]glycerol; the opposite labelling pattern, obtained by growth on [1,3-^{13}C]glycerol, is represented in green. The labelling scheme of Group I is characterized by sites either 100% or 0% enriched. In 2-SH3, for example, glycines and alanines have the alpha carbons fully labelled and the carbonyl positions unlabelled and, for the alanine, no labelling at the beta position; the opposite labelling is obtained for 1,3-SH3. Only in the case of valines and leucines, two chemically-connected carbons (the α and β for valine, and β and γ for leucine) are both fully enriched in 1,3-SH3 and both unlabelled in 2-SH3. The amino-acids of group II show a more complex labelling scheme.

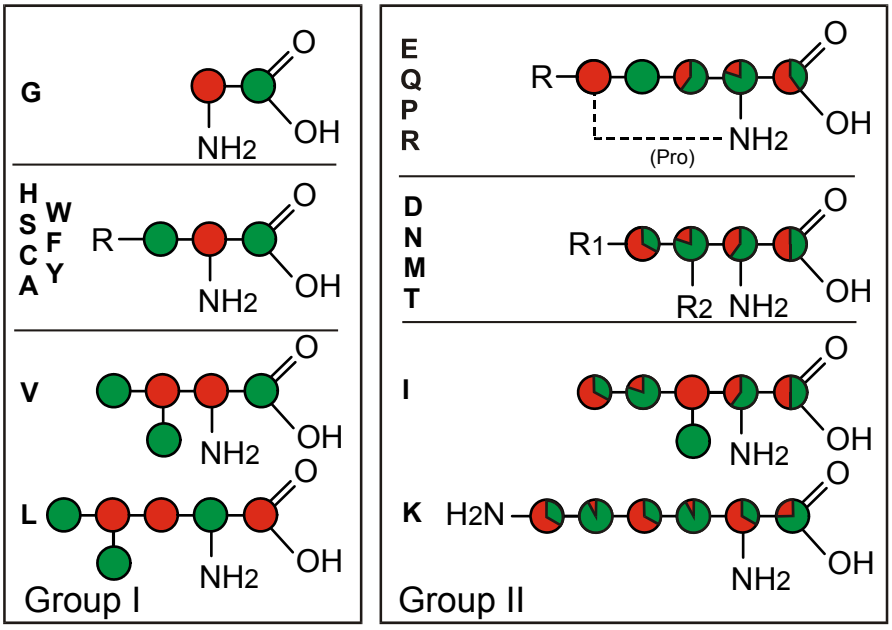

Fig. 4.2 Schematic representation of the effective ^{13}C enrichment, as obtained by protein expression in *E.coli* BL21(DE3). The red colour corresponds to the degree of ^{13}C labelling obtained by growth on [2-^{13}C] glycerol; the opposite labelling pattern, obtained by growth on [1,3-^{13}C] glycerol, is represented in green.

The strain used for the expression of the SH3 molecules is the BL21 (DE3) and contains all enzymes that are involved in the citric-acid cycle (see 4.4.1). As a consequence, the cycle can be followed several times, resulting in the production of a mixture of differently labelled molecules. On average, this results in amino-acids with nuclei partially labelled. In the figure, the percentage label from [2-^{13}C]glycerol or [1,3-^{13}C]glycerol for a particular atom is represented using relative red/green colouring. In Fig. 4.3, all the possible isotopomers produced following the citric-acid cycle several times are shown, together with the average labelling. For residues Glu, Gln, Pro and Arg five different labelled molecules can be produced. For residues Asp, Asn, Met, Thr and Ile six different isotopomers can be generated, while in the case of Lys the number increases to twelve. Looking at the average labelling of residues in Group II, it seems that for these amino-acids there are still many situations in which connected nuclei are simultaneously labelled, even if in lower percentage. This is actually not the real situation, if we consider the labelling of the single isotopomers. For every residue type, there is at least one isotopomer where each nucleus has no labelled neighbours. Especially for preparations with [2-^{13}C]glycerol, the amount of labelling is sensibly reduced and mostly alternating. Starting from [2-^{13}C]glycerol, only in the case of three isotopomers of residue Ile, two connected carbons are simultaneously labelled. The presence of a mostly alternating labelling scheme is also confirmed by different solution NMR experiments, as explained below.

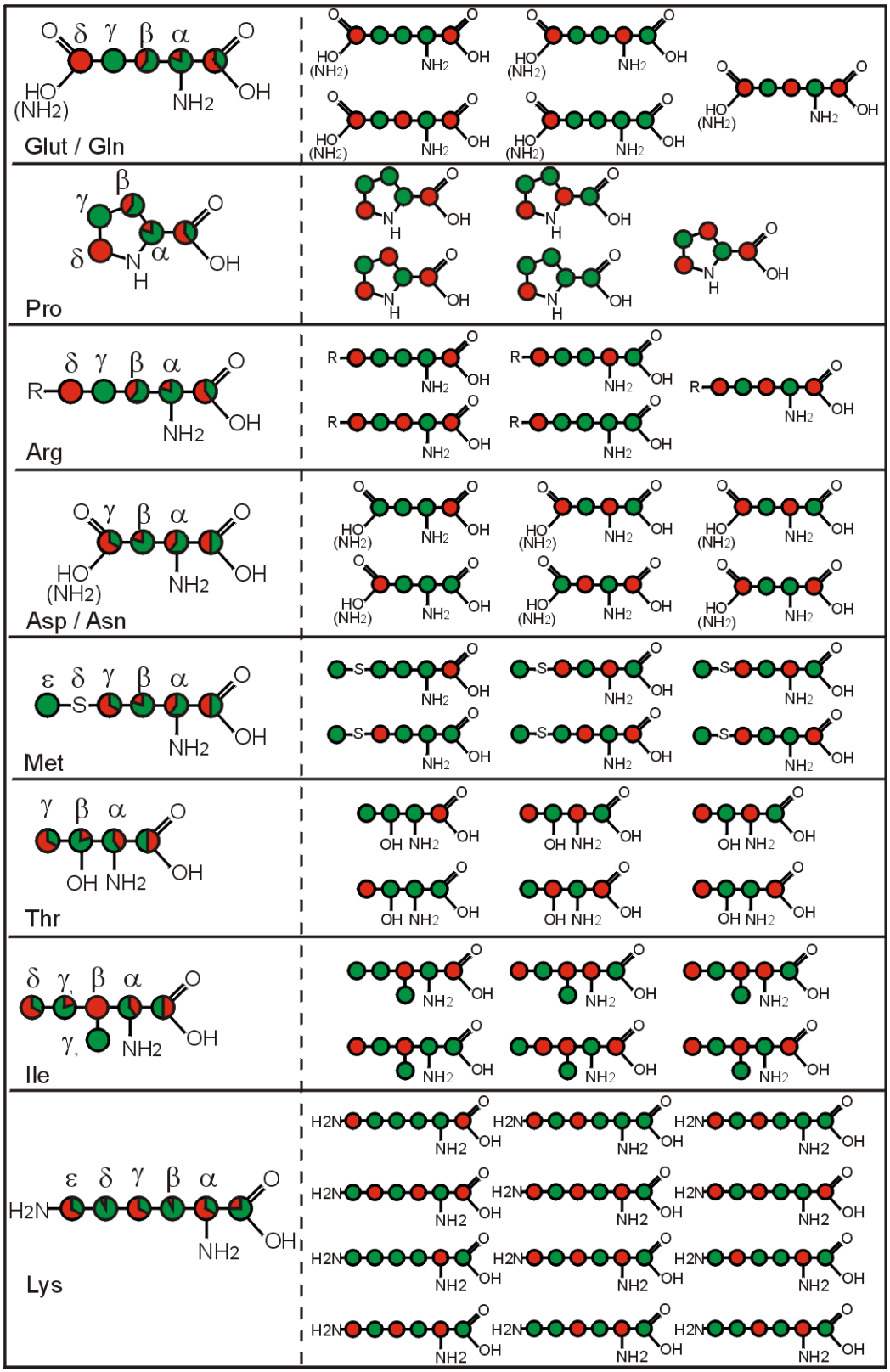

Fig. 4.3 List of the possible isotopomers produced for 10 amino-acids, which are synthesized during the cyclical reactions of the citric-acid cycle. The red colour corresponds to the degree of ^{13}C labelling obtained by growth on [2-^{13}C] glycerol; the opposite labelling pattern, obtained by growth on [1,3-^{13}C] glycerol, is represented in green.

4.2.2 Estimation of the ^{13}C labelling by solution NMR data

To verify and compare the predicted distribution of ^{13}C-enriched sites, solution NMR spectroscopy was employed. Furthermore, for residues of group II, it was not possible to estimate the relative amounts of each isotopomer produced during the biosynthetic pathway, hence the average labelling was deduced from the analysis of solution NMR spectra. The two protein samples (2-SH3 and 1,3-SH3) were dissolved in aqueous solution and different experiments were performed. The labelled carbon sites were identified by using the solution NMR chemical shifts known for this protein[8] (see Appendix A).

In Fig. 4.4, ^{15}N-^{1}H HSQC experiments[9] recorded on 2-SH3 (a) and 1,3-SH3 (b) are shown. The pulse-program was implemented in such a way to detect scalar couplings between ^{15}N amides and the connected carbonyl carbons, and to be able to derive which residues have a labelled or partially labelled CO. During the nitrogen evolution period, a selective 180º pulse on the C^{α} magnetization was applied to suppress the C^{α}-N scalar-coupling, while the CO-N coupling still evolves. Recording the spectra with high resolution, the N signal of each SH3 residue can appear as a singlet, a doublet or a mixture of the two. The singlet indicates that there are no labelled CO connected to the N, where the CO is part of the previous amino-acid. When a doublet appears, the CO of the previous amino-acid is fully enriched. In the case of a mixture of singlets and doublets, both situations are present. From the relative intensities of the singlet and doublet is also possible to derive the percentage of the labelled CO. In Fig. 4.5, the sections of the 2D ^{15}N-^{1}H HSQC spectra, indicated with dashed line in Fig. 4.4, are shown. On the side of the spectra, ^{15}N slices at ^{1}H chemical shift of 9.42 ppm illustrate the topology of the ^{15}N signals for residues L34 and L33 in the two samples. In 2-SH3 (Fig. 4.5a), the ^{15}N signal of L34 is a doublet. This means that the CO of the previous amino-acid (L33) is fully enriched, as predicted following the biosynthetic pathway. The ^{15}N signal of L33 is a mixture of a singlet and a doublet. To notice is that the singlet is not located in the centre of the doublet, but slightly shifted at lower field, because of isotope shift effects. The amino-acid that precedes is T32 and its carbonyl is only partially labelled. From the integration of the signal, the percentage of labelling is estimated ~40%. The Figure shows also the ^{15}N signal of L12 as a singlet. The previous residue is an alanine, that from the labelling prediction shouldn't have a labelled carbonyl.

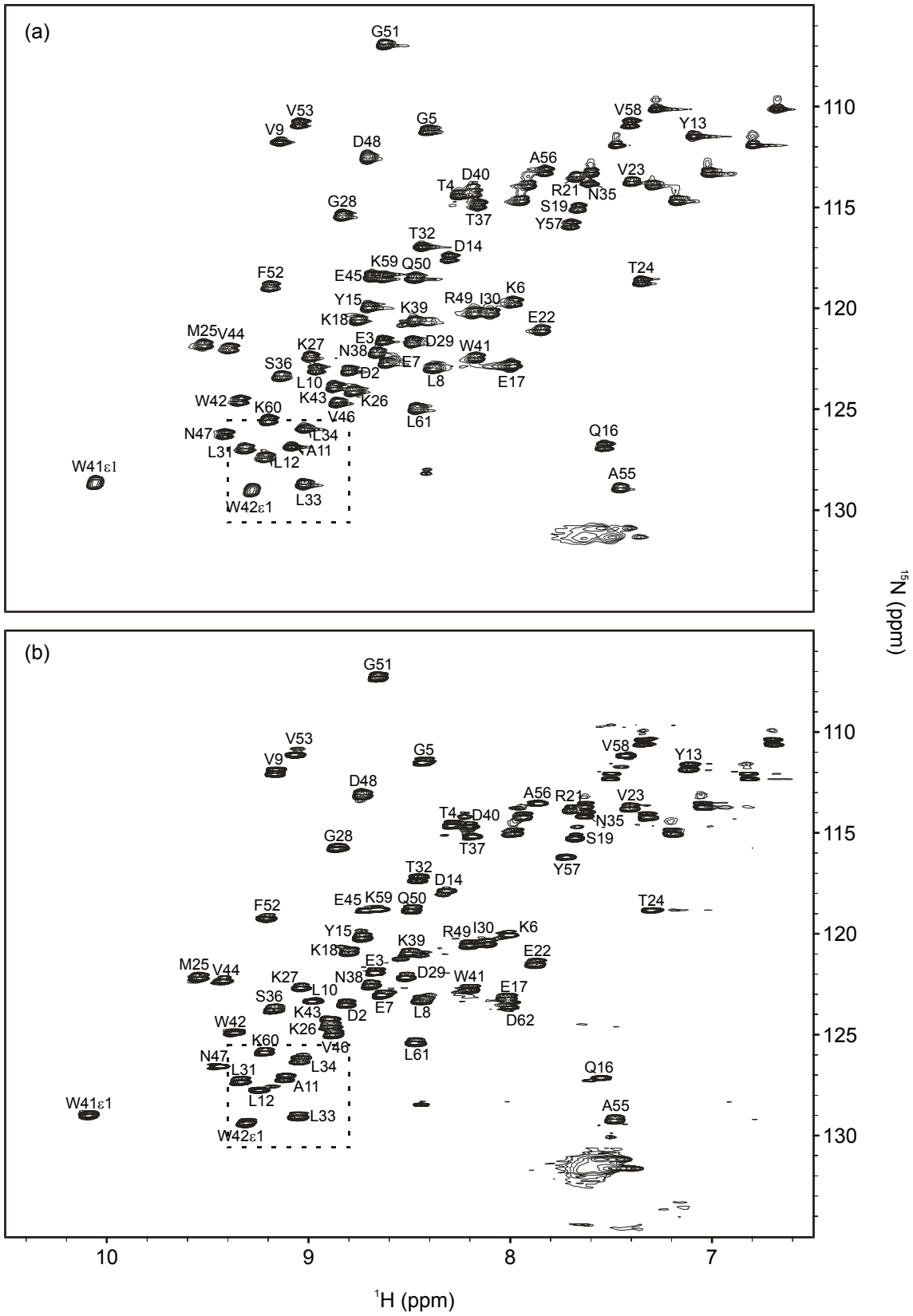

Fig. 4.4 Contour plots of ^{15}N-^{1}H HSQC experiments of 2-SH3 (a) and 1,3-SH3 (b), recorded on a DRX600 in standard configuration. During the nitrogen evolution period, a selective 180º pulse on the C^{α} magnetization suppressed the C^{α}-N scalar-coupling. The boxed regions relate to Fig. 4.5.

In Fig. 4.5b, a section of the 2D ^{15}N-^{1}H HSQC spectrum of 1,3-SH3 is depicted. In this case, the ^{15}N signal of L34 is a singlet and the ^{15}N signal of L33 a mixture of a singlet and a doublet. In this preparation, the carbonyl sites of leucines should be indeed unlabelled, while the CO of threonines should be only partially labelled. From the integration of the L33 signal, the percentage of labelled carbonyl of T32 is ~50%. The ^{15}N signal of L12 is a doublet because of the fully enriched CO of A11.

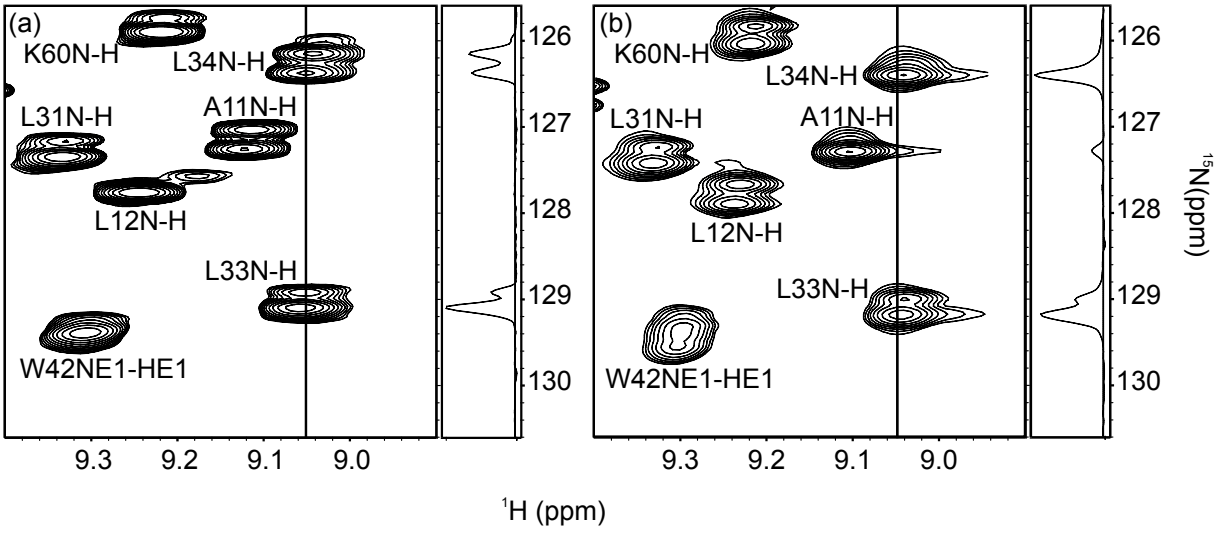

Fig. 4.5 Regions from the spectra of Fig. 4.4. On the right side of the spectra, ^{15}N slices are shown, extracted at a ^{1}H chemical shift of 9.42 ppm. From the topology of the ^{15}N signals, information about the labelling of carbonyl sites could be obtained.

2D ^{13}C-^{1}H versions of a conventional triple-resonance HNCO experiment[10] were recorded on the two samples and are reported in Fig. 4.6. In these spectra, each peak connects the ^{1}H amide chemical shift of one residue with the CO chemical shift of the previous residue. The experiments were recorded with high resolution and omitting the pulse that decouples the scalar coupling between CO and C^{α} carbons. From these spectra is possible to obtain information about the labelling of CO and C^{α} sites. Only the residues with a labelled or partially labelled CO will show respective signals in the spectra. Furthermore, from the topology of the CO signals is possible to estimate the percentage of labelling of connected C^{α} nuclei. No information are obtained about the labelling of C^{α} connected to unlabelled CO. In the spectrum of 2-SH3 (Fig. 4.6a), there are no signals corresponding to residues Gly, Ser, Trp, Phe, Tyr, Ala and Val, as expected. Moreover, all the detected signals appear as singlets. This means that in none of the isotopomers there is a labelled C^{α} connected to a labelled CO. This is in agreement with our prediction, as shown in Fig. 4.3. In the spectrum of 1,3-SH3

(Fig. 4.6b) six signals are not present, corresponding to leucines. The detected peaks are mostly mixtures of singlets and doublets, except in the case of Gly, Ser, Trp, Phe, Tyr, Ala and Val which are pure singlets, because of unlabelled C^{α}.

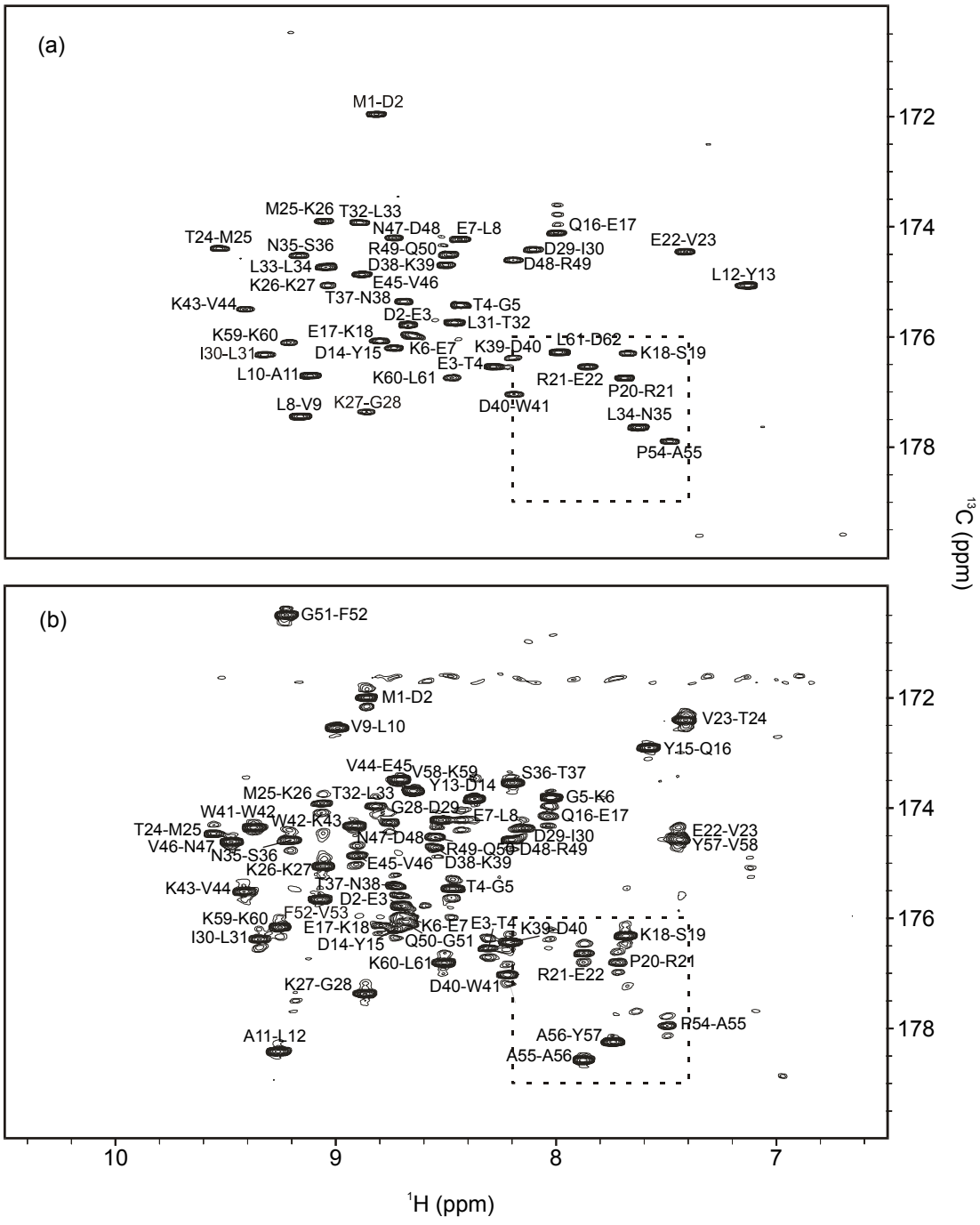

Fig. 4.6 Contour plots of 2D ^{13}C-^{1}H spectra of a conventional triple-resonance HNCO experiment recorded on a DRX600 in standard configuration, for 2-SH3 (a) and 1,3-SH3 (b). The experiments were recorded with high resolution and omitting the pulse that decouples the scalar coupling between CO and C^{α} carbons. The boxed regions relate to Fig. 4.7.

In Fig. 4.7 the regions of the spectra indicated in Fig. 4.6 are shown. On the side, ^{13}C slices at ^{1}H chemical shift of 7.86 ppm illustrate the topology of the CO signals of R21. In 2-SH3 (Fig. 4.7a), this signal is a singlet, while in 1,3-SH3 (Fig. 4.7b) is a mixture of singlet and doublet. By integration of these signals, it results that in 1,3-SH3 the percentage of labelled C^{α} of R21 connected to labelled CO is ~50%. Among the six possible isotopomers produced in the citric-acid cycle for Arg, two molecules have a labelled CO and in only one of these two molecules the labelled CO is connected to a labelled C^{α}. In the same ^{13}C slice, the signal of A55 appears as a singlet, confirming the absence of C^{α} labelling for this type of residue. The CO signal of A55 is missing in the spectrum of 2-SH3 (Fig. 4.7a), meaning no labelling for alanine CO.

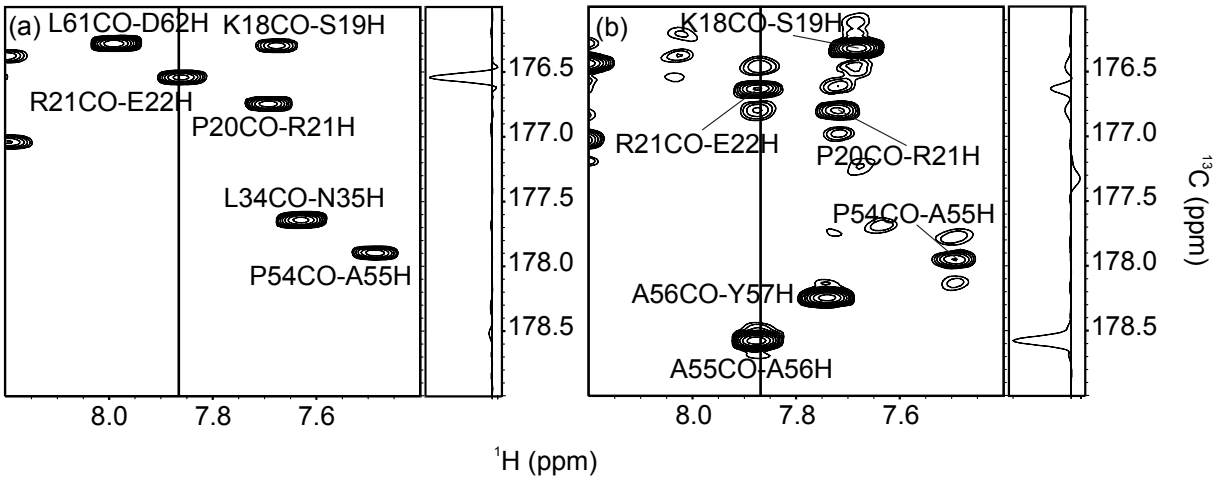

Fig. 4.7 Regions from the spectra of Fig. 4.6. On the right side of the spectra, ^{13}C slices are shown, extracted at a ^{1}H chemical shift of 7.86 ppm. From the topology of the ^{13}CO signals, information about the labelling of connected C^{α} nuclei could be obtained.

In order to get information about the labelling of C^{β} sites, 2D ^{13}C-^{1}H versions of a conventional triple-resonance HNCA experiment[10] were performed on the two samples, as shown in Fig. 4.8. In this experiment, the ^{1}H amide chemical shift of one residue is correlated with the C^{α} chemical shift of the same and previous residues. The spectra were recorded with high resolution, to be able to resolve scalar-couplings with C^{β} nuclei and hence get information about their labelling. The coupling to the CO is suppressed via a 180º pulse on the CO magnetization during ^{13}C evolution. In Fig. 4.8a the spectrum recorded on 2-SH3 is depicted. The signals of the valines and of I30 appear as doublets. In this preparation, the valine residues have both C^{α} and C^{β} fully enriched. In the case of I30, the C^{α} is labelled only in two isotopomers, which have also C^{β} labelled. The other signals are singlets. This is in

agreement with the predicted isotopomers for 2-SH3, that never have a labelled C^{α} followed by a labelled C^{β}, except in the case of valine and isoleucine residues.

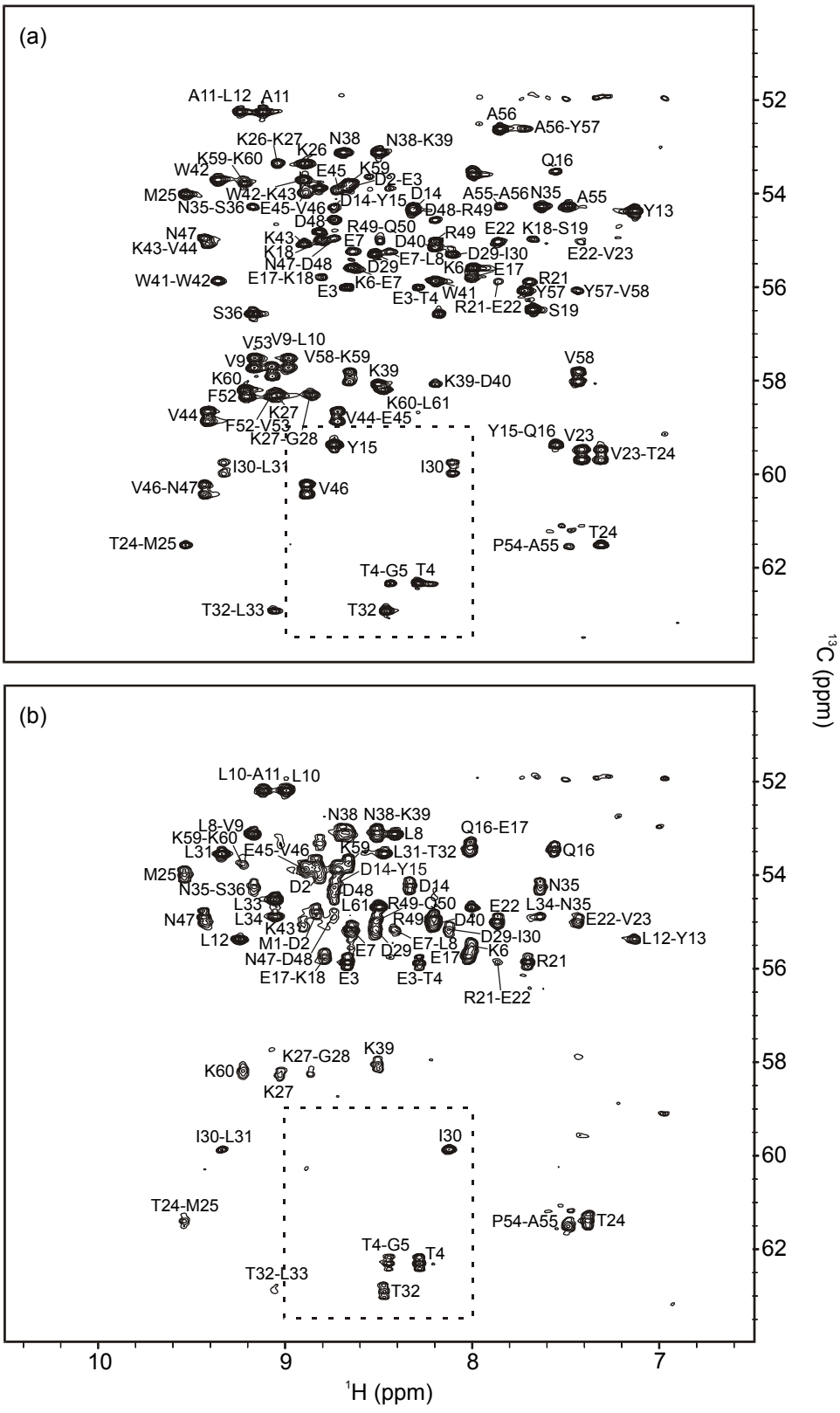

Fig. 4.8 Contour plots of 2D ^{13}C-^{1}H spectra of a conventional triple-resonance HNCA experiment recorded on a DRX600 in standard configuration, for 2-SH3 (a) and 1,3-SH3 (b). The spectra were recorded with high-resolution. The boxed regions relate to Fig. 4.9.

In Fig. 4.9 the regions indicated with dotted lines in Fig. 4.8 are reproduced. The ^{13}C slices at ^{1}H chemical shift of 8.28 ppm illustrate the topology of the C^{α} signals of T4. In 2-SH3 (Fig. 4.9a), this signal is a singlet and in 1,3-SH3 (Fig. 4.9b) a mixture of singlet and doublet. From integration, the amount of labelled C^{β} connected to labelled C^{α} is estimated to be ~60%. Four of the six possible isotopomers produced in the case of threonine have a labelled C^{α}. Three of these four isotopomers have a labelled C^{β} connected to the labelled C^{α}.

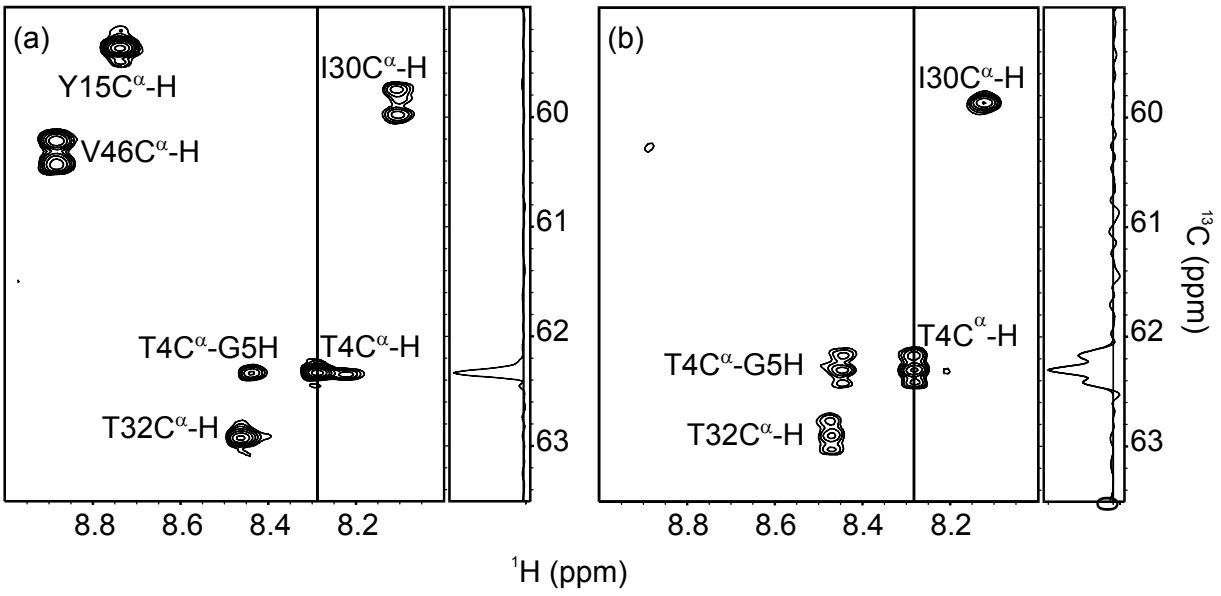

Fig. 4.9 Regions from the spectra of Fig. 4.8. On the right side of the spectra, ^{13}C slices are shown, extracted at a ^{1}H chemical shift of 8.28 ppm. From the topology of the $^{13}C^{\alpha}$ signals, information about the labelling of connected C^{β} nuclei could be obtained.

In Fig. 4.10, two different aminoacid-selective experiments, each of them recorded on the two protein preparations, are shown. In these experiments a selective transfer step for NH_2 groups[11] is implemented at the beginning of conventional triple-resonance HNCA (a and b) and HNCO (c and d) experiments[10] to create aminoacid-selective pulse sequences for Asn and Gln residues. In the spectra in (a) and (b), recorded on 2-SH3 and 1,3-SH3 respectively, each peak correlates the ^{1}H chemical shifts of NH_2 groups of Asn and Gln with the ^{13}C chemical shifts of C^{β} of Asn and C^{γ} of Gln. In (a) only signals of Asn are present, indicating that the C^{γ} of Gln are never labelled in 2-SH3. In (b) all the signals corresponding to Asn and Gln residues of the SH3 are present, indicating that C^{β} of Asn and C^{γ} of Gln are fully or partially ^{13}C enriched in 1,3-SH3. Analysing the spectra in (c) and (d), information on the labelling of C^{γ} of Asn and C^{δ} of Gln is obtained. These spectra are recorded combing the selective transfer step for NH_2 groups with an HNCO experiment. Furthermore, the experiments were recorded

with high resolution and setting to zero the power of the pulse that decouples the scalar coupling between the side-chain carbonyl and the connected carbons.

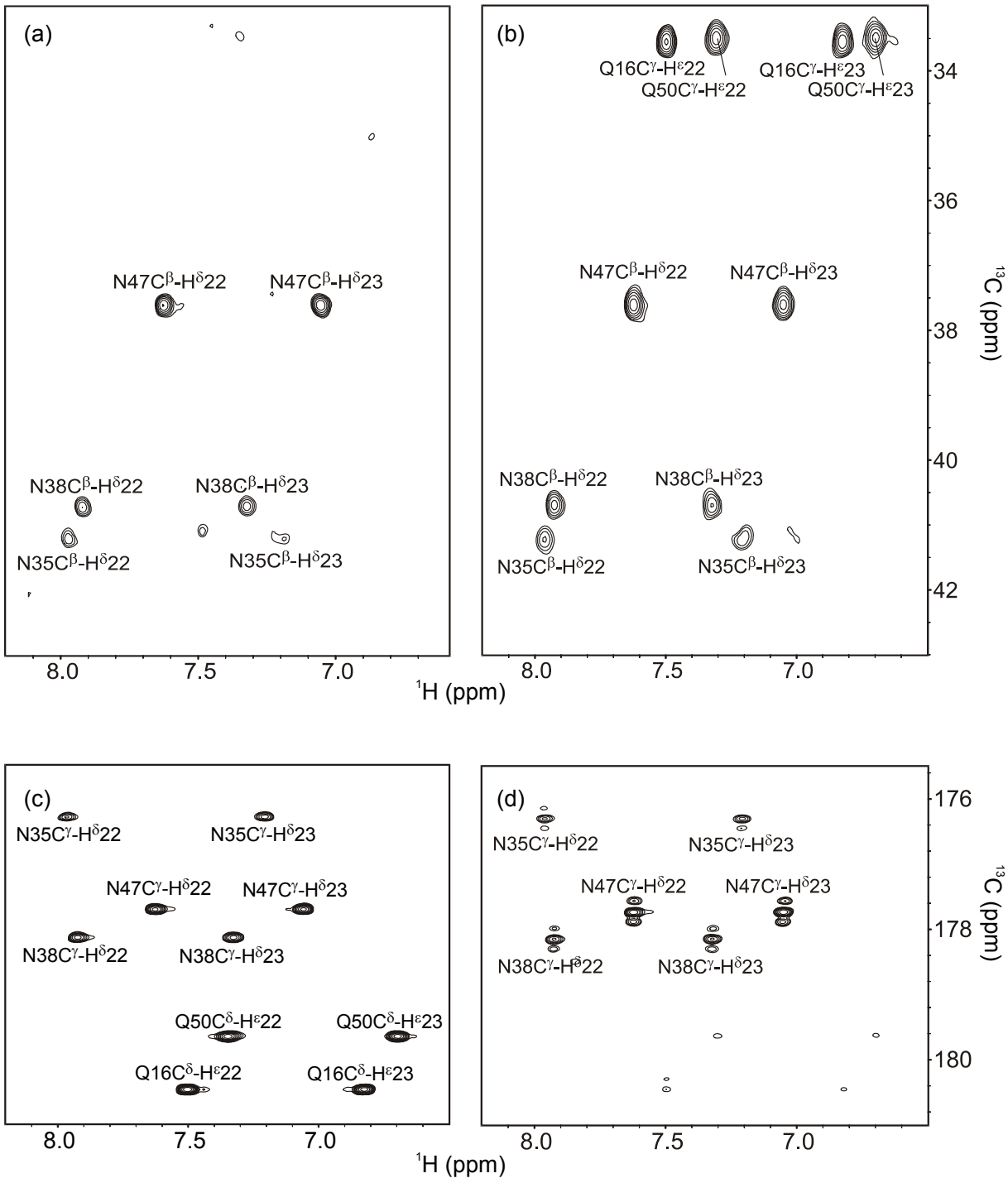

Fig. 4.10 Asn/Gln selective experiments. The spectra in (a) and (b) are obtained combining a selective transfer step for NH_2 groups[11] at the beginning of a conventional triple-resonance HNCA experiment, recorded on 2-SH3 and 1,3-SH3, respectively. Signals belonging to C^{β} of Asn and C^{γ} of Gln are detected. The spectra in (c) for 2-SH3 and in (d) for 1,3-SH3, are obtained implementing a selective transfer step for NH_2 groups[11] at the beginning of a conventional triple-resonance HNCO experiment. Signals due to C^{γ} of Asn and C^{δ} of Gln are detected.

For 2-SH3 (c), all the signals of C^{γ} of Asn and C^{δ} of Gln are present. The topology of the ^{13}C signals provides information on the labelling of the connected nuclei. All peaks appear as singlets, indicating that no labelled nuclei are connected to these sites. For 1,3-SH3 (d), only signals of C^{γ} of Asn are detected and they are resolved in a mixture of a singlet and a doublet. In 1,3-SH3, two of the six isotopomers of Asn have labelled C^{γ} and in one case the labelled C^{γ} is connected to a labelled C^{β}.

In Fig. 4.11a and b, sections of high resolution ^{1}H-^{13}C HSQC spectra[12,13] are shown, recorded on 2-SH3 and 1,3-SH3, respectively. The analysis of the topology and intensity of each peak of these spectra allowed us to complete the estimation of labelling in each carbon site of the two protein preparations. The labelling scheme is summarized in Fig. 4.2. Overall, the predicted labelling patterns are in good agreement with the information obtained by the solution NMR spectra. Moreover, it seems that all the possible isotopomers of the amino-acid of group II are produced and essentially in equal amount.

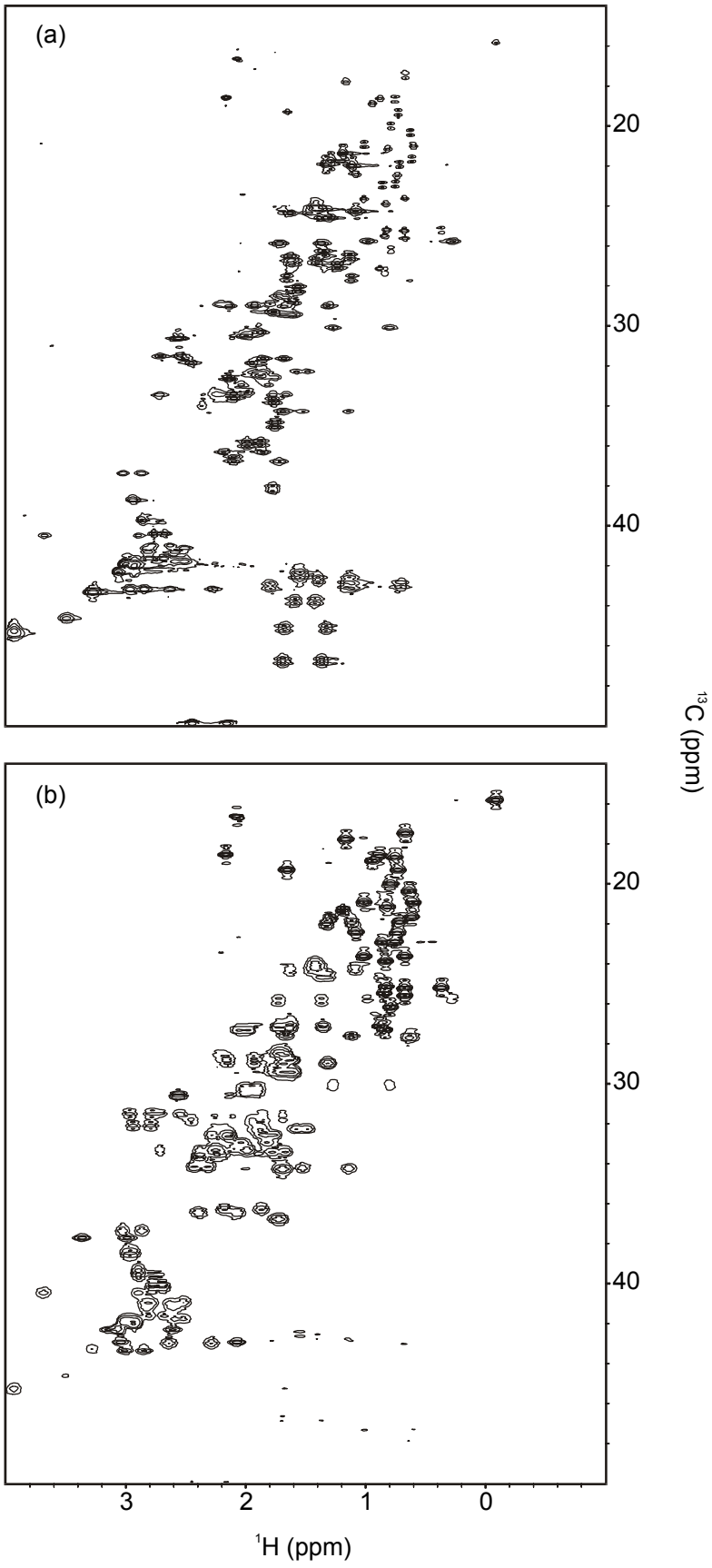

Fig. 4.11 Contour plots of high-resolution ^{13}C-HSQC spectra of 2-SH3 (a) and 1,3-SH3 (b), recorded on a DRX600 in standard configuration.

4.3 Improvement in resolution in 2-SH3 and 1,3-SH3 spectra

An important and advantageous side-effect of the alternating ^{13}C-labelling is that the carbon lines in ^{13}C CP/MAS NMR spectra of 2-SH3 and 1,3-SH3 are significantly narrower with respect to spectra recorded on uniformly ^{13}C enriched samples. The reduced labelling partly suppresses or completely removes line-broadening due to ^{13}C-^{13}C scalar-couplings. These effects are illustrated in Fig. 4.12, in which 1D ^{13}C CP/MAS spectra of (U-^{13}C)-SH3 (a), 2-SH3 (b) and 1,3-SH3 (c) are compared.

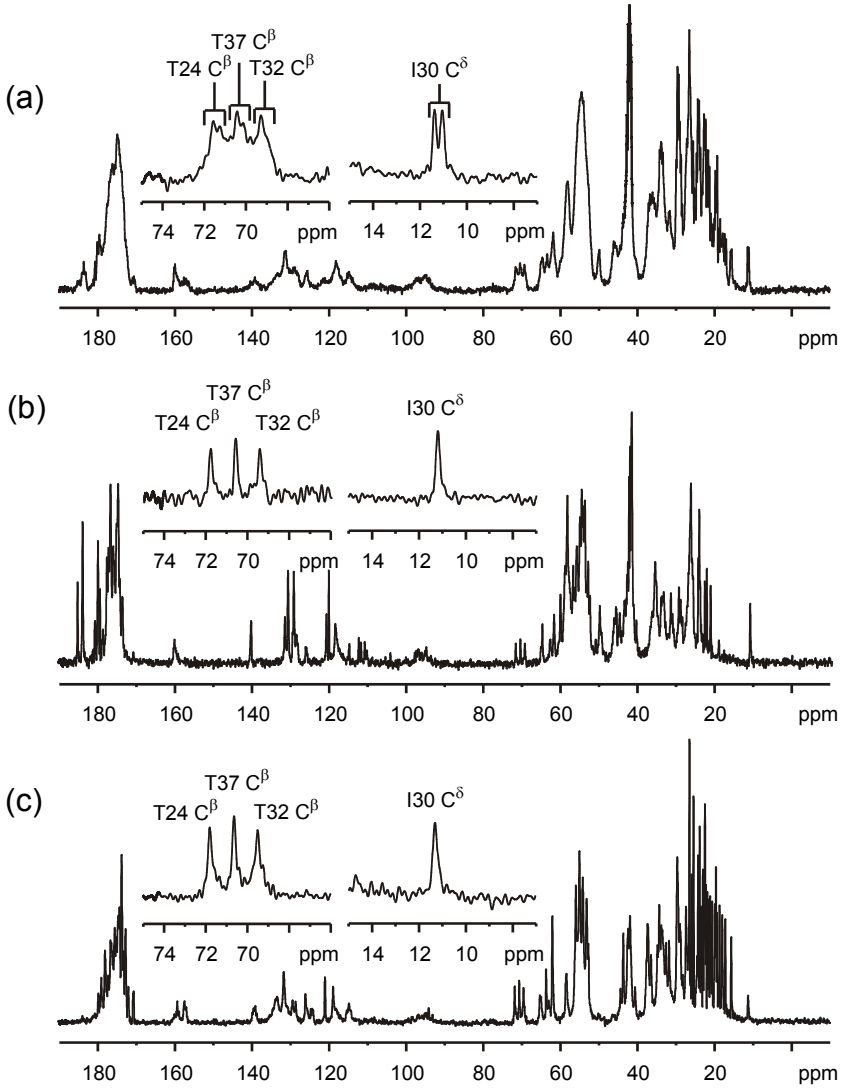

Fig. 4.12 1D ^{13}C CP-MAS spectra of (U-^{13}C)-SH3 (a), 2-SH3 (b) and 1,3-SH3 (c) recorded at 9.4 T and using a spinning frequency of 8.0 kHz. The spectra are recorded with a long acquisition time of 45 ms and 64 scans. In the expansions of the C^{β} signals of threonines and the C^{δ} signal of I30, the line-widths obtained with the different ^{13}C labelling schemes can be compared.

The insets show the well-resolved C^{δ} signal of I30 at 11.3 ppm and the C^{β} signals from three threonines around 70 ppm. Substantial broad lines are observed in the (U-^{13}C)-SH3 sample (a); for a relatively short acquisition time of ~25ms, the signals of I30 C^{δ} and threonine C^{β} have line-widths of 60-70Hz (data not shown). For longer acquisition times (e.g. 45 ms), the signal of I30 C^{δ} can be resolved in a doublet, due to the scalar coupling with the neighbouring $C^{\gamma 1}$ (a). The signals of the threonine C^{β} present a more structured feature due to multiple couplings to both α and γ carbons (a). In the 2-SH3 sample, these signals have line-widths of 20-25 Hz (b). The remarkable narrowing of these resonances in comparison to the fully enriched SH3 arises from the fact that in none of the isotopomers of the isoleucine (see Fig. 4.3), the C^{δ} and $C^{\gamma 1}$ are labelled at the same time, which completely removes the one-bond ^{13}C-^{13}C scalar-coupling broadening. The same is observed for the C^{β} of threonine, that never is connected to a ^{13}C-labelled neighbour (see Fig. 4.3). In case of 1,3-SH3, a situation is observed, where in some of the isotopomers (see Fig. 4.3) the C^{δ} atom of I30 and the C^{β} atoms of threonines are connected with labelled carbons. In the 1D spectrum the line-width of these signals are 30-35 Hz (c).

For assignment strategies and structure-determination concepts, different experiments need to be performed. In particular, homonuclear ^{13}C-^{13}C dipolar correlation experiments are used to identify the single amino-acids[14-17] and heteronuclear ^{15}N-^{13}C dipolar correlation experiments are necessary for the sequential assignment[16-21]. A selection of experiments was recorded on a uniformly ^{13}C-enriched SH3 and on the two biosynthetically site-directed ^{13}C-labelled SH3 preparation, to evaluate the effect of the labelling on the resolution of the spectra. In Fig. 4.13, 2D ^{15}N-^{13}C dipolar correlation spectra are shown, recorded on (U-^{13}C)-SH3 (a,b), 2-SH3 (c,d) and 1,3-SH3 (e,f). The spectra on the left side (a, c, e) are NCO type and are obtained using a specific-CP step[22], to transfer selectively magnetization from the amide ^{15}N to the ^{13}CO of the previous residue. On the right (b, d, f), NCA type of spectra are depicted, obtained by selective transfer of magnetization from the amide ^{15}N to $^{13}C^{\alpha}$ of the same residue. For (U-^{13}C)-SH3 (a,b), peaks corresponding to almost all residues of the SH3 are detected and assigned, even if the spectra show in some extend problems of overlap. Remarkable improvement in resolution is achieved for 2-SH3 and 1,3-SH3, due to both ^{13}C line-narrowing and reduced spin-labelling. Signals corresponding to residues of the Group I are missing in either NCO or NCA spectra, because of lack of labelling in CO or C^{α} sites.

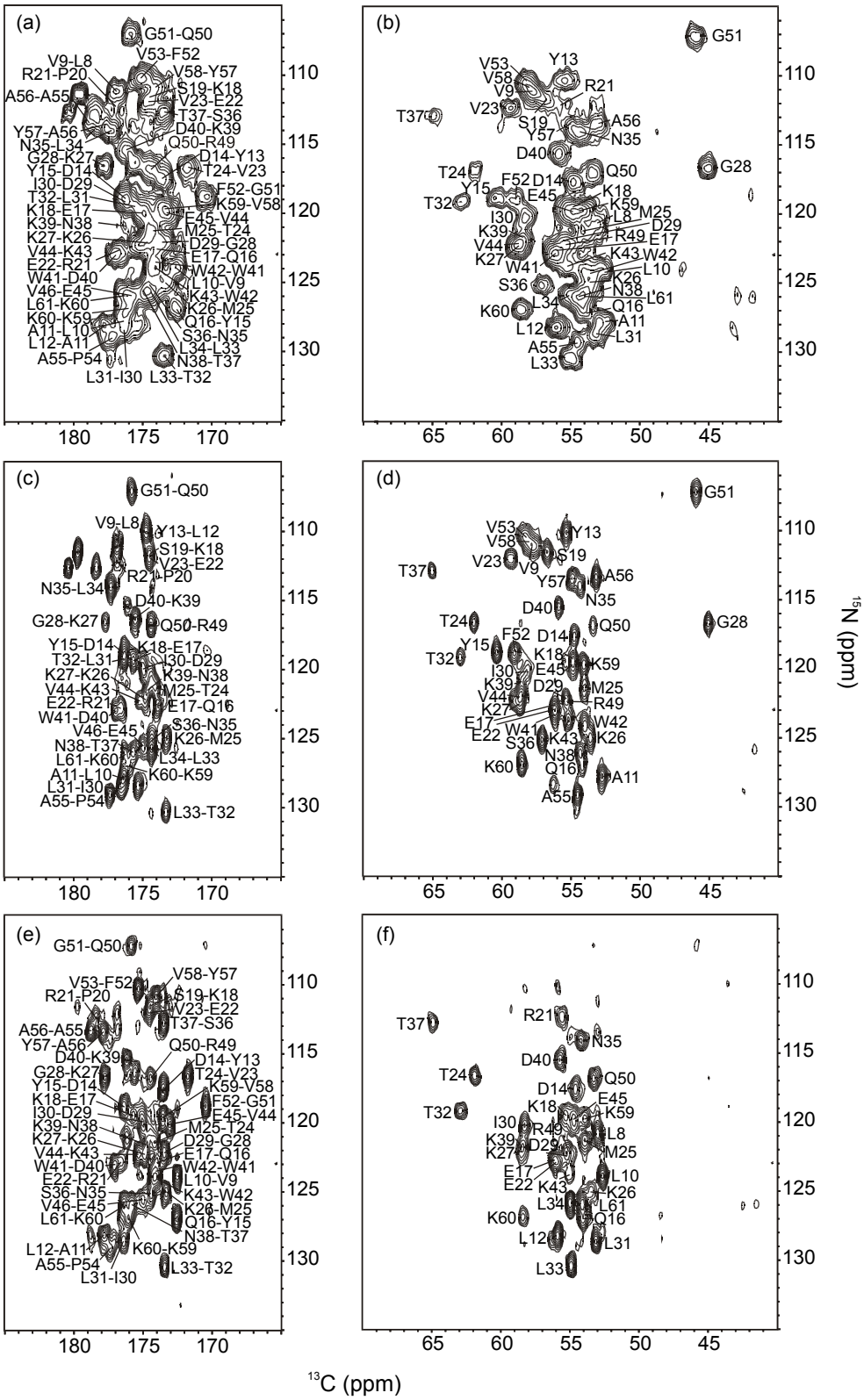

Fig. 4.13 In (a), (c) and (e) 2D NCO spectra are shown, recorded on (U-^{13}C)-SH3, 2-SH3 and 1,3-SH3, respectively. On the right side, 2D NCA spectra are shown, recorded on (U-^{13}C)-SH3 (b), 2-SH3 (d) and 1,3-SH3 (f). All the spectra are recorded at 9.4 T and using a spinning frequency of 8.0 kHz. The selective transfer of magnetization from ^{15}N amides to C^{α} or CO carbons is achieved via a specific-CP step, obtained by applying weak *rf*-fields, on resonance with the ^{15}N amides in ^{15}N channel and off-resonance in the ^{13}C channel.

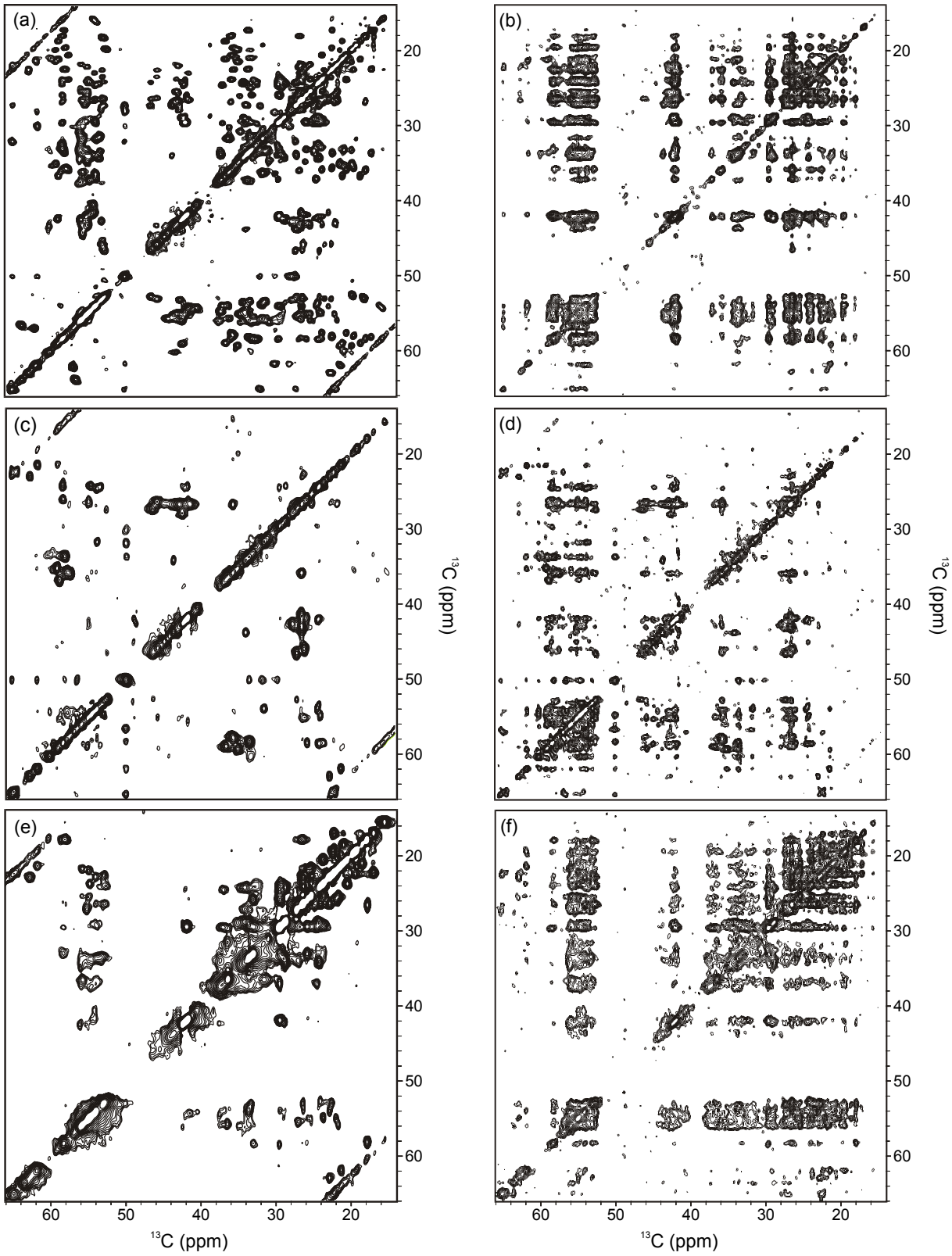

Fig. 4.14 2D ^{13}C-^{13}C PDSD spectra recorded on (U-^{13}C)-SH3 (a,b), 2-SH3 (c,d) and 1,3-SH3 (e,f). The spectra on the left side are acquired using a short mixing time of 15 ms for (U-^{13}C)-SH3 (a) and of 50 ms for 2-SH3 (c) and 1,3-SH3 (e). The spectra on the right side are all recorded with a long mixing time of 500 ms. All the spectra are recorded at 17.6 T and using a spinning frequency of 8.0 kHz.

The resolution enhancement obtained for biosynthetically site-directed ^{13}C-labelled preparations, would be particularly important in the case of solid-state NMR investigations of larger systems.

In Fig. 4.14, 2D ^{13}C-^{13}C dipolar correlation experiments are shown, recorded using the broad-band proton-driven spin-diffusion (PDSD) recoupling scheme[23]. The spectra on the left are acquired using a short mixing time and can be used for assignment purposes. In the PDSD spectrum of (U-^{13}C)-SH3 (a), intra-residue peaks are detected and assigned. In the case of our protein, no problems of overlap are encountered, due to the relatively small size of the system. In the case of 2-SH3 (c) and 1,3-SH3 (e), less peaks are detected because of the reduced labelling. The dilution of labelling simplifies the spectra and may facilitate the assignment of larger solid proteins. Increasing the mixing time to 500 ms new peaks are observed, as shown in the spectra (b), (d) and (f) of Fig. 4.14. In the case of 2-SH3 (d) and 1,3-SH3 (f), because of the reduction of dipolar truncation and spin-diffusion effects, many of the new peaks are assigned to long-range correlations and used to get structure information on the system, as discuss more extensively in Chapter 5.

4.4 Materials and methods

4.4.1 Sample preparation

The SH3 protein was expressed in *Escherichia coli* BL21 (DE3), using M9 minimal media. Plasmid pET3d coding for α-spectrin SH3 protein from chicken brain was a generous gift of Dr. M. Saraste (EMBL, Heidelberg). For (U-^{13}C,^{15}N)-SH3, 1.5 g of [U-^{13}C] glucose and 1.0 g $^{15}NH_4Cl$ per litre of medium were added[15]. A total of 0.5 g $^{15}NH_4Cl$, 2.0 g $NaH^{12}CO_3$ and 2.0 g [1,3-^{13}C] glycerol per litre of medium were used in the case of ([1,3-^{13}C] glycerol, ^{15}N) SH3[7]. For the preparation of the ([2-^{13}C] glycerol, ^{15}N) SH3 sample, 0.5 g $^{15}NH_4Cl$, 2.0 g $NaH^{13}CO_3$ and 2.0 g [2-^{13}C] glycerol were added[7]. The proteins were purified by anion exchange chromatography (Q-Sepharose FF, Amersham Pharmacia Biotech), gel filtration (Superdex 75 pg, Amersham Pharmacia Biotech) and dialysis. The final yield was approximately 20 mg of protein per litre of culture. A 200 mM $(NH_4)_2SO_4$ solution (pH 3.5, 0.04% NaN_3) was added to a 1.15 mM SH3 solution (pH 3.5) at a volume ratio of 1:1. The protein samples for MAS measurement were precipitated by changing the pH to a value of 7.5

in NH3 atmosphere. The solution was kept in a refrigerator (4ºC) overnight before the precipitate was separated and centrifuged inside 4-mm CRAMPS rotors.

4.4.2 Solution NMR spectroscopy

For the solution NMR measurements, approximately 3 mg of protein was dissolved in 300 µl water solution (pH 3.5) and a shigemi tube was used. All the solution NMR spectra were recorded at room temperature (300 K) on a Bruker DRX-600 spectrometer operating at a proton frequency of 600.13 MHz.

The ^{15}N-HSQC spectra[9] were recorded with 512 (t1) × 512 (t2) complex points in each dimension and spectral width of 3012 Hz (^{15}N) × 10000 Hz (^{1}H). The total acquisition time was 1.5 hours, using 4 scans. A 180º pulse on the $^{13}C^{\alpha}$ magnetization was applied during nitrogen evolution.

The 2D ^{13}C-^{1}H versions of a conventional triple-resonance HNCO experiment[10] were recorded with 128 (t1) × 512 (t2) complex points in each dimension and spectral width of 2778 Hz (^{13}C) × 10000 Hz (^{1}H). The total acquisition time was 45 minutes, using 8 scans. No C^{α} decoupling was applied during ^{13}CO evolution, to be able to detect scalar coupling between C^{α}-CO nuclei.

The 2D ^{13}C-^{1}H versions of a conventional triple-resonance HNCA experiment[10] were recorded with 128 (t1) × 512 (t2) complex points in each dimension and spectral width of 2778 Hz (^{13}C) × 10000 Hz (^{1}H). The total acquisition time was 45 minutes, using 8 scans.

The Asn/Gln selective experiments to detect signals from C^{β} of Asn and C^{γ} of Gln were obtained implementing a selective transfer step for NH_2 groups[11] at the beginning of a conventional triple-resonance HNCA experiment[10]. 128 (t1) × 512 (t2) complex points in each dimension were recorded with spectral width of 1667 Hz (^{13}C) × 10000 Hz (^{1}H). The total acquisition time was 1.5 hours, using 16 scans.

The Asn/Gln selective experiments to detect signals from C^{γ} of Asn and C^{δ} of Gln were obtained implementing a selective transfer step for NH_2 groups[11] at the beginning of a conventional triple-resonance HNCO experiment[10]. 128 (t1) × 512 (t2) complex points in each dimension were recorded with spectral width of 1667 Hz (^{13}C) × 10000 Hz (^{1}H). For this experiment, no ^{13}C decoupling was applied during ^{13}C evolution to detect coupling with neighbouring carbons. The total acquisition time was 1.5 hours, using 16 scans.

The high-resolution ^{13}C-^{1}H HSQC spectra[12,13] were recorded with 512 (t1) × 512 (t2) complex points in each dimension and spectral width of 10000 Hz (^{13}C) × 10000 Hz (^{1}H). The total acquisition time was 1.5 hours, using 4 scans.

All the solution data were processed were processed with the XWINNMR software, version 2.6 (Bruker, Karlsruhe, Germany) and subsequently analysed using the program Sparky, version 3.100 (T.D. Goddard & D.G. Kneller, University of California).

4.4.3 Solid-state NMR spectroscopy

For the MAS measurements, approximately 6-7 mg of protein was used and confined to the centre of 4 mm rotors by use of spacers. The 2D ^{15}N-^{13}C heteronuclear dipolar correlation experiments were performed on a DMX-400 spectrometer (Bruker, Karlsruhe, Germany) operating at a field of 9.4 T and equipped with a 4 mm triple-resonance CP/MAS probe (Bruker, Karlsruhe, Germany). The datasets were recorded at 280 K and at MAS frequency $\omega_R/2\pi$ = 8.0 kHz. Fore NCA experiments, the magnetization is selectively transferred from nitrogen to the C^{α} atoms while for NCO experiments, the magnetization transfers from ^{15}N to the carbonyl atoms. For both experiments the same pulse sequence was applied. Following ^{1}H excitation, a ramped cross polarization contact of 500 μs between ^{1}H and ^{15}N created the initial ^{15}N magnetization; spin lock fields were 33 kHz for ^{1}H and 19-26 kHz for the ^{15}N ramp. Following the nitrogen evolution, specific-CP[22] was employed to selectively transfer magnetization from ^{15}N to $^{13}C^{\alpha}$, in the case of NCA, and from ^{15}N to ^{13}CO, in the case of for NCO. In both experiments, weak RF powers corresponding to nutation frequencies of ~10 kHz for the ^{15}N and ~20 kHz for the ^{13}C were used and the amide ^{15}N were irradiated close to resonance while the $^{13}C^{\alpha}$ and ^{13}CO off-resonance. The ^{13}C frequency offset was varied to match the appropriate NCA or NCO specific-CP condition. During the evolution periods, proton decoupling was applied, using the two-pulse phase modulation technique (TPPM)[24], with a pulse width of 7.3 μs and a 10˚ phase modulation. The 2D datasets were acquired using 2494×160 points and dwell times of 10 μs and 100 μs for f2 and f1, respectively; each FID was averaged from 16 scans, using a 3 s recycle delay, yielding a total measurement time of ~2 hours for each 2D experiment.

The 2D ^{13}C-^{13}C PDSD experiments were performed at a field of 17.6 T on a DMX-750 narrow-bore spectrometer, equipped with a 4 mm double-resonance MAS probe (Bruker,

Karlsruhe, Germany). Ramped cross polarization from ^{1}H to ^{13}C created the initial transverse carbon magnetization; spin-lock fields were 36 kHz for ^{1}H and 18–36 kHz for the ^{13}C ramp. After the first ^{13}C evolution period, carbon magnetization was exchanged by using a PDSD mixing scheme[23]. Spin diffusion periods of 15–500 ms were applied. Typical carbon 90° pulse lengths were 5.3 μs. A proton RF field of ~60 kHz was applied for the two-pulse phase modulation decoupling during ^{13}C acquisition and evolution. The 2D ^{13}C-^{13}C spectra were recorded with 32–64 scans, and with ~ 6 ms evolution in the indirect dimension, leading to experimental times of 16 to 32 hours.

All the solid-state data were processed with the XWINNMR software, version 2.6 (Bruker, Karlsruhe, Germany) and subsequently analysed using the program Sparky, version 3.100 (T.D. Goddard & D.G. Kneller, University of California).

References

1. Lehninger, A. L., Nelson, D. L., & Cox, M. M. (1993). *Principles of Biochemistry* Worth Publishers, New York.

2. Stryer, L. (1995). *Biochemistry* W.H. Freeman, New York.

3. Hong, M. & Jakes, K. (1999). Selective and extensive 13C labeling of a membrane protein for solid-state NMR investigations. *J. Biomol. NMR* **14**, 71-74.

4. LeMaster, D. M. & Kushlan, D. M. (1996). Dynamical mapping of E-coli thioredoxin via C-13 NMR relaxation analysis. *J. Am. Chem. Soc.* **118**, 9255-9264.

5. Hodgkinson, P. & Emsley, L. (1999). The accuracy of distance measurements in solid-state NMR. *J. Magn. Reson.* **139**, 46-59.

6. Kiihne, S., Mehta, M. A., Stringer, J. A., Gregory, D. M., Shiels, J. C., & Drobny, G. P. (1998). Distance measurements by dipolar recoupling two-dimensional solid-state NMR. *Journal of Physical Chemistry A* **102**, 2274-2282.

7. Castellani, F., van Rossum, B., Diehl, A., Schubert, M., Rehbein, K., & Oschkinat, H. (2002). Structure of a protein determined by solid-state magic-angle-spinning NMR spectroscopy. *Nature* **420**, 98-102.

8. Blanco, F. J., Ortiz, A. R., & Serrano, L. (1997). 1H and 15N NMR assignment and solution structure of the SH3 domain of spectrin: comparison of unrefined and refined structure sets with the crystal structure. *J. Biomol. NMR* **9**, 347-357.

9. Sklenar, V., Piotto, M., Leppik, R., & Saudek, V. (1993). Gradient-Tailored Water Suppression for ^{1}H-^{15}N HSQC Experiments Optimized to Retain Full Sensitivity. *J. Magn. Reson. A* **102**, 241-245.

10. Ikura, M., Kay, L. E., & Bax, A. (1990). A novel approach for sequential assignment of 1H, 13C, and 15N spectra of proteins: heteronuclear triple-resonance three-dimensional NMR spectroscopy. Application to calmodulin. *Biochemistry* **29**, 4659-4667.

11. Schmieder, P., Leidert, M., Kelly, M., & Oschkinat, H. (1998). Multiplicity-Selective Coherence Transfer Steps for the Design of Amino Acid-Selective Experiments-A Triple-Resonance Experiment Selective for Asn and Gln. *J. Magn Reson.* **131**, 199-202.

12. Bodenhausen, G. & Ruben, D. J. (1980). *Chem. Phys. Lett.* **69**, 185-189.

13. Mueller, L. (1979). *J. Am. Chem. Soc.* **101**, 4481-4484.

14. McDermott, A., Polenova, T., Bockmann, A., Zilm, K. W., Paulson, E. K., Martin, R. W., Montelione, G. T., & Paulsen, E. K. (2000). Partial NMR assignments for uniformly (13C, 15N)-enriched BPTI in the solid state. *J. Biomol. NMR* **16**, 209-219.

15. Pauli, J., van Rossum, B., Forster, H., de Groot, H. J. M., & Oschkinat, H. (2000). Sample optimization and identification of signal patterns of amino acid side chains in 2D RFDR spectra of the alpha-spectrin SH3 domain. *J. Magn. Reson.* **143**, 411-416.

16. Hong, M. (1999). Resonance assignment of 13C/15N labeled solid proteins by two- and three-dimensional magic-angle-spinning NMR. *J. Biomol. NMR* **15**, 1-14.

17. Egorova-Zachernyuk, T. A., Hollander, J., Fraser, N., Gast, P., Hoff, A. J., Cogdell, R., de Groot, H. J., & Baldus, M. (2001). Heteronuclear 2D-correlations in a uniformly [13C, 15N] labeled membrane-protein complex at ultra-high magnetic fields. *J. Biomol. NMR* **19**, 243-253.

18. Fujiwara, T., Sugase, K., Kainosho, M., Ono, A., Ono, A., & Akutsu, H. (1995). C-13-C-13 and C-13-N-15 Dipolar Correlation Nmr of Uniformly Labeled Organic-Solids for the Complete Assignment of Their C-13 and N-15 Signals - An Application to Adenosine. *J. Am. Chem. Soc.* **117**, 11351-11352.

19. Sun, B. Q., Rienstra, C. M., Costa, P. R., Williamson, J. R., & Griffin, R. G. (1997). 3D N-15-C-13-C-13 chemical shift correlation spectroscopy in rotating solids. *J. Am. Chem. Soc.* **119**, 8540-8546.

20. Pauli, J., Baldus, M., van Rossum, B., de Groot, H., & Oschkinat, H. (2001). Backbone and side-chain C-13 and N-15 signal assignments of the alpha-spectrin SH3 domain by magic angle spinning solid-state NMR at 17.6 tesla. *Chembiochem* **2**, 272-281.

21. Jaroniec, C. P., MacPhee, C. E., Astrof, N. S., Dobson, C. M., & Griffin, R. G. (2002). Molecular conformation of a peptide fragment of transthyretin in an amyloid fibril. *Proc. Natl. Acad. Sci. U. S. A* **99**, 16748-16753.

22. Baldus, M., Petkova, A. T., Herzfeld, J., & Griffin, R. G. (1998). Cross polarization in the tilted frame: assignment and spectral simplification in heteronuclear spin systems. *Mol. Phys.* **95**, 1197-1207.

23. Szeverenyi, N. M., Sullivan, M. J., & Maciel, G. E. (1982). Observation of Spin Exchange by Two-Dimensional Fourier-Transform C-13 Cross Polarization-Magic-Angle Spinning. *J. Magn. Reson.* **47**, 462-475.

24. Bennett, A. E., Rienstra, C. M., Auger, M., Lakshmi, K. V., & Griffin, R. G. (1995). Heteronuclear decoupling in rotating solids. *J. Chem. Phys.* **103**, 6951-6958.